



Received on 03 November 2020; received in revised form, 06 December 2020; accepted, 23 December 2020; published 01 January 2021

CANDIDATURE OF THE SYNTHETIC CASPASE INHIBITORS AS NEW ANTI-SARS-COV-2 DRUG DISCOVERY, *IN-SILICO* MOLECULAR DOCKING

Adham M. M. Zaki ^{*1}, Yasmin Moustafa Ahmed ² and El-Shimaa M. N. Abdelhafez ³

Department of Medicinal Chemistry ¹, Faculty of Pharmacy ³, Minia University - 61519, Minia, Egypt.

Department of Pharmacology and Toxicology ², Nahda University, Beni Suef Governorate, Egypt.

Keywords:

3C-like protease,
SARS coronavirus, Drug Discovery,
Caspases, Molecular docking

Correspondence to Author:

Adham M. M. Zaki

Department of Medicinal Chemistry,
Faculty of Pharmacy, Minia
University - 61519, Minia, Egypt.

E-mail: adham_zaki@pharm.s-mu.edu.eg

ABSTRACT: The new pandemic virus identified as severe acute respiratory syndrome Coronavirus 2 is the etiological agent responsible for the pneumonia outbreak that ended with respiratory failure. The main protease (M^{PRO}) is a key enzyme for SARS-CoV-2, which plays a pivotal role in mediating viral replication and transcription, making it an attractive drug target for this virus. Here, we determine the mechanism-based for binding and interactions between the reported caspase inhibitors and M^{PRO}, by computer-aided drug design molecular docking. In addition to the prediction of physicochemical properties, pharmacokinetics, and drug-likeness profile *in-silico* as well as reviewing the previously reported antiviral activity of the caspase inhibitors and how could the viruses get an advantage from the apoptosis process. Molecular operating environment is used for docking between thirteen reported caspase inhibitors compounds and SARS-COV-2 main protease using HWH (~{N}- [2- (5- fluoranyl-1~ {H}-indol-3-yl) ethyl] ethanamide) as a reference. The results have shown that almost all of the reported anti-caspase compounds revealed acceptable binding with good docking scores and favorable *in-silico* pharmacokinetic profile that might promise a rapid discovery of drug leads with clinical potential in response to new infectious diseases for which no specific drugs or vaccines are available.

INTRODUCTION: In November 2002, in Guangdong Province, China, a virus known as SARS-CoV was identified and involved in the extreme acute respiratory syndrome. By December 2019, after seventeen years coronavirus was identified again from Wuhan, china which able to transmit from human to human as an aerosol infection then causes severe acute respiratory syndrome corona virus (SARS-CoV-2) ¹.

In December 2020, SARS-CoV-2 had infected more than 65 million cases and 1, 501, 350 deaths across 213 countries ². Coronaviruses are enveloped positive - sense single-stranded RNA viruses of 30 kb ³. It subdivided into four genera; α , β , γ and δ based on their genomic structure, α and β genera are a wide variety of host species infected mammals ⁴⁻⁵.

Lymphocyte such as cytotoxic T cells and nature killer cells are playing an important role in viral infection management ⁶. From what's been happening lately, it seems like lymphopenia is the major diagnostic inductor of SARS-COV-2 infection ⁷, where lymphocytes are depleted as a direct result of virus-induced apoptosis which

<p>QUICK RESPONSE CODE</p> 	<p>DOI: 10.13040/IJPSR.0975-8232.12(1).104-19</p> <hr/> <p>This article can be accessed online on www.ijpsr.com</p> <hr/> <p>DOI link: http://dx.doi.org/10.13040/IJPSR.0975-8232.12(1).104-19</p>
---	--

causes suppression of immune response leading to combat viral infection along with a wide infection spread rate inside the body, multiple organ failures, and increase of mortality rate⁸⁻⁹.

Mechanism of Human Immune Response against SARS-COV-2 and SARS-COV-2 Pathogenesis:

Inflammatory Cytokines Role: The innate immune system can recognize the molecular structures that are produced by the invasion of the virus, which is called pathogen-associated molecular patterns (PAMPs)¹⁰. Coronavirus is considered RNA virus where PAMPs are founded in the shape of viral genomic double-stranded RNA which are recognized by several events lead to activation of specific signaling pathways such as nuclear factor (NF- κ B), activator protein 1 (AP-1), interferon response factor 3 (IRF3), IRF7 lead to stimulation of many molecules which required for inflammatory responses, including inflammatory cytokines (e.g., [TNF] tumor necrosis factor and IL-1). Interferon type I (IFN- α and IFN- β) production is promoted by IRF3 and IRF7, which are important for the antiviral activity of the innate immunity and ultimately able to suppress viral replication at an early stage. This process can cause complications such as cough, exhaustion, and weakness in patients¹¹.

In the case of SARS-COV-2 infection, low-grade fever and cough are moderate signs although approximately 15% of cases are related to respiratory compromise; on the opposite hand, severe cases lead to acute respiratory distress syndrome (ARDS) with systemic inflammation within which lung injury is related to the discharge of inflammatory cytokines which plays a very important role in immunopathology during infection¹².

There is significant literature implicating the delayed release of cytokines and chemokines occurs in respiratory epithelial cells, dendritic cells (DCs), and macrophages at SARS-COV-2 early stages of infection¹³. However, within the late stages, the cells secrete low levels of the antiviral factors interferon's (IFNs) and high levels of (IL)-1 β , IL-6, tumor necrosis factor (TNF), CCL-2, CCL-3, and CCL-5¹⁴⁻¹⁵. Recent literature implicating that the Nod-like receptor family pyrin

domain containing 3 (NLRP3) inflammasome and cytokine storm together plays an important role in SARS-COV-2 activation of innate immunity to recognize pathogens in viral infections pathogenesis¹⁶⁻¹⁷. However, we SARS-COV 3aprotein activates the NLRP3 in lipopolysaccharide-primed macrophages with 3a-mediated IL-1 β secretion associated with K⁺ efflux and mitochondrial reactive oxygen species (ROS)¹⁸. By contrast, SARS-COV-2 patients with mild symptoms were experienced lower levels of IL-6, together with activated T lymphocytes and IgM SARS-CoV-2- binding antibodies¹⁵. The recent studies reported an increase in inflammatory cytokine response mediates severe disease; however, the low responses are also related to an adaptive response that favors disease resolution¹⁹. The response of immunity to production IFN-I or IFN- α/β reflects the key natural immune defense response against viral infection, as IFN-I is that the fundamental molecule that has an important role mechanism as an antiviral within the early stages of viral infection²⁰. In the early SARS-COV-2 infection, delayed IFNs release delays the body antiviral response. Later, the rapid increase in both cytokines and chemokines appeal to several inflammatory cells leading to excessive infiltration of the inflammatory cells resulting in tissue injury²¹.

These studies indicate that the unorganized and overproduction of both cytokine and chemokine and IFN-I delayed responses by SARS-CoV-infection that would play an important role in the pathogenesis of SARS-2, looks as If lymphopenia is that the major diagnostic inductor of SARS-COV-2 infection⁷, where lymphocytes are depleted as a direct result of virus-induced apoptosis²² which causes suppression on immunologic response resulting in combat viral infection together with a large infection spread rate inside the body, multiple organ failures and increase of mortality rate⁹.

Apoptosis between Immunity and SARS-COV-2 Infection Strategies: Apoptosis or programmed cell death is one of the processes that regulate many cellular functions such as homeostasis between multicellular organisms and limit viral spreading across human cells²³. It could be a common host cell response against viral infection

as it limits viral spreading by removing infected cells²⁴. A family of cytokines called interferons plays a significant role within the regulation of apoptosis by stimulating cytotoxic T cells (CTLs) and many intracellular genes that directly induce apoptosis and prevent virus replication²⁵. Viruses that encode anti-apoptotic protease are likely to inhibit the apoptosis process to facilitate its replication and spreading²⁶. Several similar viruses encode Bcl-2 homologs, which inhibit activation of apoptotic caspases and block the death of the host cell²⁷ as well as interfering with other pro-apoptotic molecules, for example papillomavirus E7 and HHV-8 that encodes several versions of the IRFs, which interferes with normal IRF function²⁸. Many viruses take advantage of apoptosis to facilitate its replication²⁷; the major protein involved in the apoptosis process is a family of cysteine-dependent aspartate-directed proteinases called caspases²⁹. Caspases have a vital role in diverting non-apoptotic processes like migration and differentiation²⁷, the lytic infection by virus-induced apoptosis leads to the formation of apoptotic bodies that are absorbed by neighboring cells, which help in dissemination progeny as well as limiting immune responses³⁰.

Structural Proteins Implicate Caspase Induced Apoptosis by SARS-COV-2: SARS-CoV-2 has four main structural proteins, Spike (S), Envelope

(E), Nucleocapsid (N), and M membrane (M)³¹. SARS-COV-N protein cleavage is essential for viral replication, which depends on host cell caspase cleavage³²⁻³³.

The more surprising correlation is with SARS-COV-2 infected cells upon treatment with pan-caspase inhibitor Z-VAD-FMK N-protein cleavage were also inhibited because of the reduction in viral replication³³.

Membrane Protein: SARS-CoV-2 membrane protein is considered the most concentrated protein in viral envelope³⁴. The M protein facilitates membrane fusion and controls viral replication; furthermore, viral packaging RNA in matured virions³⁵. It has been demonstrated that M is abundant within the Golgi body of viral-infected cells³⁶ inductions of apoptosis by overexpression of M protein in HPF cells are reported³⁷. M protein induces apoptosis in host cells by activates caspase 3-8 and -9.

Moreover, over-expression of the M protein results in down-regulation of Akt phosphorylation as shown in **Fig. 1**, which reducing cell survival signal and induced apoptosis; additionally, mislocalization of mitochondrial cytochrome C and nuclear condensation was observed in M-expressing cells³⁸⁻³⁹.

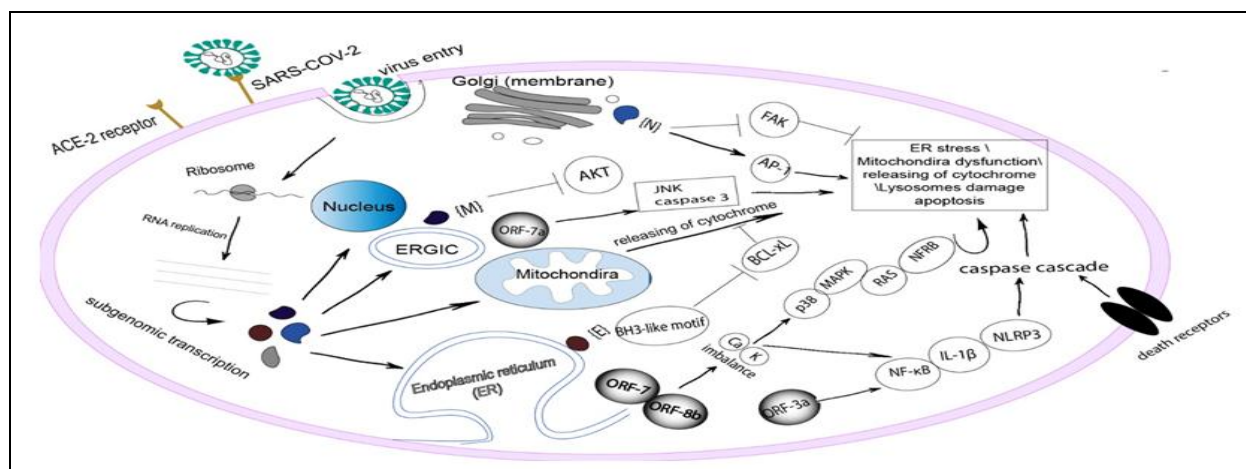


FIG. 1: THE DIAGRAM IS SHOWING THE DYNAMIC INTERACTION NETWORK BETWEEN SARS-COV-2 AND HOST CELL WHICH INVOLVING S-GLYCOPROTEIN BINDING TO THE ACE2 RECEPTOR, WHICH ENHANCING VIRAL ENTRY VIA ENDOCYTOSIS AND SUBSEQUENT UN-COATING AND RELEASING VIRAL GENOME. CELLULAR FUNCTIONS IN VARIOUS COMPARTMENTS (CYTOPLASM, PLASMA MEMBRANE, ER, GOLGI, ERGIC NUCLEUS, AND MITOCHONDRIA) MAY BE INTERFERED WITH SARS-COV-2 PROTEINS EVENTUALLY LEAD TO ACTIVATION OF CASPASE CASCADE, ER STRESS, MITOCHONDRIA DYSFUNCTION, RELEASING OF CYTOCHROME. THE ABBREVIATION: ANGIOTENSIN-CONVERTING ENZYME 2 (ACE2), THE ENDOPLASMIC-RETICULUM-GOLGI INTERMEDIATE COMPARTMENT (ERGIC), THE OPEN READING FRAME (ORF) 7A, C-JUN N-TERMINAL KINASES (JNKs), B-CELL LYMPHOMA-EXTRA-LARGE (BCL-XL), NUCLEAR FACTOR KAPPA-LIGHT-CHAIN-ENHANCER OF ACTIVATED B CELLS NF-KB, FOCAL ADHESION KINASE (FAK), A MITOGEN-ACTIVATED PROTEIN KINASE (MAPK)

Nucleocapsid Protein: SARS coronavirus N protein is a pro-apoptotic protein; it regulates activation of many pathways like virus life cycles, cell proliferation, host cell apoptosis⁶, AP-1 signal transduction pathway, caspase-3, -7 and 9⁴²⁻⁴⁰. The N protein cleavage is essential for viral replication³². The mechanism of activation of caspase cascade by N protein is not clear, but it was reported that N protein activates apoptosis through activation of mitochondria pathway by increasing the release of cytochrome C and ROS into cytosol⁴³. Interestingly, the Caspase-3,-6 are involved in N protein cleavage, which explains why are viral replication reduced upon the addition of pan-caspase inhibitor Z-VAD-FMK³³. However, the mechanism is not fully known, but there is two possibilities either N is translocated into the nucleus, leading to the activation of caspase-6 or N can be imported into the nucleus only if caspase-6 is involved during apoptotic processes⁴⁴. Also, down-regulation of FAK (focal adhesion kinase) and fibronectin expression by SARS-CoV have been reported⁴⁰.

SARS-CoV-2 Envelope Protein: SARS-CoV-2E protein shares high sequence similarities to SARS-CoV-1 E protein, which is strongly conserved in N-term regions and it is the smallest of all 8–12 kDa structural proteins⁴⁵⁻⁴⁶. SARS-CoV-2 E proteins share a conserved Bcl-2 Homology 3 (BH3)-like motif in their C-terminal region; a well-studied motif shown to be necessary for SARS-CoV E binding to Bcl-xL47; it has been found that apoptosis is promoted by Ectopic expression of SARS-CoV E³¹.

Accessory Proteins Implicate Caspase Induced Apoptosis by SARS-COV-2: Eight putative accessory proteins are encoded on the SARS-Co V genome (ORFs 3a, 7a, 3b, 7b, 6, 8a, 9b and 8b), which does not have any homologs⁴⁸. In other words, there are three main SARS-CoV-2 accessory proteins involved in the induction of apoptosis⁴⁹.

First, ORF-3a (also called U2 74, SARS X1, or ORF-3) is suggested to be located in several sub-cellular compartments as its multifunctional protein 50 causes caspase 8 cleavages to facilitate nuclear translocation of viral component⁵¹ and ultimate maturation of viral particles⁴⁹⁻⁵².

On the other hand, ORF-3b, also called ORF-4, which is a predominantly localized protein in the nucleolus and partially in the mitochondria, plays a role in G0/G1 arrest and apoptosis indication in transfected cells⁵³. ORF-7a (also known as X4 or ORF-8) that encodes a type I transmembrane protein located in the cell surface and Golgi apparatus⁵⁴⁻⁵⁵, consisting of a 15 residue N-terminal signal peptide, an 81 residue luminal domain, a 21 residue transmembrane segment, 122 amino acid and a 5 residue cytoplasmic tail⁵⁵. ORF-7a not only induce apoptosis but also inhibit cellular protein synthesis through activating p38 mitogen-activated protein kinase (MAPK) signaling pathway, activate NF-κB56, block cell cycle progression, and interact with the cellular transcription factor small glutamine-rich tetratricopeptide repeat-containing protein (SGT); furthermore the anti-apoptotic regulator Bcl-XLthis could imply that the induction of apoptosis by these different proteins occurs at different stages of the infection cycle⁵⁷⁻⁵². The encoding of these pro-apoptotic proteins on the SARS-COV-2 genome suggests that apoptosis is useful for the cleavage of viral protease, which facilitates SARS-COV-2 replication⁵⁸.

Main Protease (MPRO): SARS-COV-2 Main protease (MPRO) or chymotrypsin-like cysteine protease named 3C-like protease (3CLpro) enzymes are required for translation of polyprotein from viral RNA⁵⁹ and viral replication⁶⁰. The auto-cleavage of polyprotein to 1a and 1ab by main protease and papain-like protease is essential for SARS-COV maturation and replication; also, caspase-3 cleavage is considered as the most important step on polyprotein cleavage⁶¹. Therefore, it would be suggested that inhibiting the caspase-3 enzyme would block viral replication⁶². The MPRO Inhibitors are unlikely to be toxic as no reported human protease with the identical cleavage specificity is known⁶³. A significant increase in ROS level and inhibition of AP1-dependent transcription, likewise as activation of NF-κB-dependent reporter caspase-3 and caspase-9 on the cell expressing SARS-CoV 3CLpro was reported⁶⁴ which induct that 3CLpro activate a series of signaling events ultimately leading to programmed cell death or apoptosis induced by SARS-COV-2⁶⁵.

The Antiviral Activity of Caspases Inhibitors:

TABLE 1: CASPASE INHIBITORS AND THEIR ANTIVIRAL ACTIVITY WITH THEIR 2D STRUCTURE IN SEVERAL RECORDED STUDIES DEMONSTRATING THE ROLE OF CASPASE INHIBITORS AS ANTIVIRAL ACTIVITY

Compound Name	Structure/ Iupac Name	Antiviral Effect
Z-FA-FMK	compound 1 benzyl N-[(2S)-1-[(4-fluoro-3-oxobutan-2-yl)amino]-1-oxo-3-phenylpropan-2-yl]carbamate	It selectively inhibits caspases 2, 3, 6 and irreversible inhibitor of cysteine proteases like cathepsins B, L, and S Which caused a reduction in reovirus orthoreovirus (PRV) replication as well as aquareovirus (CSRV), and rhabdovirus (IHNV) replication ^{66, 67-68}
Z-VAD-FMK	compound 2 methyl (3S)-5-fluoro-3-[[[(2S)-2-[[[(2S)-3-methyl-2-(phenylmethoxycarbonylamino)butanoyl]amino]propanoyl]amino]-4-oxopentanoate	A pan-caspase inhibitors, which inhibit the proteolytic activity of the CVB3 proteases 2A and 3C which cause a reduction on both viral RNA and viral proteins ⁶⁹
Q-VD-OPH	compound 3 (3S)-5-(2,6-difluorophenoxy)-3-[[[(2S)-3-methyl-2-(quinoline-2-carboxylamino)butanoyl]amino]-4-oxopentanoic acid	A pan-caspase inhibitors, which suppress the release of newly produced CVB3 from infected cells which suppressed the production of viral progeny ⁷⁰
Z-LEHD-FMK	compound 4 methyl (4S)-5-[[[(2S)-1-[(3S)-5-fluoro-1-methoxy-1,4-dioxopentan-3-yl]amino]-3-(1H-imidazol-5-yl)-1-oxopropan-2-yl]amino]-4-[[[(2S)-4-methyl-2-(phenylmethoxycarbonylamino)pentanoyl]amino]-5-oxopentanoate	A caspase 9 inhibitor, inhibits the proapoptotic activity of SADS-CoV-271 and reduce the replication of HIV-1, and SADS-CoV-2 ^{71, 72-73}
IETD-FMK	compound 5 (4S)-4-[[[(2S,3S)-2-amino-3-methylpentanoyl]amino]-5-[[[(2S,3R)-1-[[[(2S)-1-carboxy-4-fluoro-3-oxobutan-2-yl]amino]-3-hydroxy-1-oxobutan-2-yl]amino]-5-oxopentanoic acid	A caspase 8 inhibitor produced modest inhibition of apoptosis and subsequent HIV-1 replication as well as it preserves and maintains HIV-1-specific immune responses ⁷²⁻⁷⁴
Z-ASP-CH2-DCB	compound 1 (3S)-5-(2,6-dichlorobenzoyl)oxy-4-oxo-3-(phenylmethoxycarbonylamino) pentanoic acid	A caspase-3 inhibitor that significantly reduced the replication of highly pathogenic avian influenza virus A/FPV/Bratislava/79 (H7N7) and calicivirus ⁷⁵⁻⁷⁶

Ac-DEVD-CHO		A caspase-3 inhibitor responsible for a pronounced inhibition of ADV viral genomic replication, gene expression on and viral titer 51 A caspase-3 inhibitor
Z-YVAD-fmk	compound 2 (4S)-4-[[[(2S)-2-acetamido-3-carboxypropanoyl]amino]-5-[[[(2S)-1-[[[(2S)-1-carboxy-3-oxopropan-2-yl]amino]-3-methyl-1-oxobutan-2-yl]amino]-5-oxopentanoic acid	A Caspase-1 inhibitor that reduced oncolytic herpes simplex virus replication and oncolytic herpes simplex virus ⁷⁷
Z-VEID-FMK	compound 8 methyl (3S)-5-fluoro-3-[[[(2S)-2-[[[(2S)-2-[[[(2S)-3-(4-hydroxyphenyl)-2-(phenylmethoxycarbonylamino)propanoyl]amino]-3-methylbutanoyl]amino]propanoyl]amino]-4-oxopentanoate	A Caspase-6 inhibitor which preventing an Arbovirus from acquiring a replicative advantage by delayed mosquito bites as well as it induced cutaneous innate immune responses 78. Also, it reduced the classic swine fever virus replication ⁵¹⁻⁷⁸
Z-WEHD-FMK	compound 9 methyl (4S)-5-[[[(2S,3S)-1-[[[(3S)-5-fluoro-1-methoxy-1,4-dioxopentan-3-yl]amino]-3-methyl-1-oxopentan-2-yl]amino]-4-[[[(2S)-3-methyl-2-(phenylmethoxycarbonylamino)butanoyl]amino]-5-oxopentanoate	A caspase-1 inhibitor which rescued more than half of the cells undergoing HCV- PCD and inhibits HCV replication ⁷⁹
Z-DEVD-FMK	compound 10 methyl (4S)-5-[[[(2S)-1-[[[(3S)-5-fluoro-1-methoxy-1,4-dioxopentan-3-yl]amino]-3-(1H-imidazol-5-yl)-1-oxopropan-2-yl]amino]-4-[[[(2S)-3-(1H-indol-3-yl)-2-(phenylmethoxycarbonylamino)propanoyl]amino]-5-oxopentanoate	It is a caspase-3 inhibitor that was used for reducing SARS-COV dissemination by inhibiting caspase-3 activation caused by the ORF-6 induced apoptosis pathway 80. Furthermore, Z-DEVD-FMK inhibits Fowl Adenovirus Serotype 4 (FAdV4) replication ⁸¹
	compound 11 methyl (4S)-5-[[[(2S)-1-[[[(3S)-5-fluoro-1-methoxy-1,4-dioxopentan-3-yl]amino]-3-methyl-1-oxobutan-2-yl]amino]-4-[[[(2S)-4-methoxy-4-oxo-2-(phenylmethoxycarbonylamino)butanoyl]amino]-5-oxopentanoate	

METHODS AND RESULTS:

Molecular Docking Results: Ligand-protein docking was carried out for all reported compound 1-13 and N-[2-(5-fluorenyl-1H-indol-3-yl)ethyl] ethanamide (HWH) 14 as a reference for the purpose of prediction the binding interactions between all reported caspase inhibitor (anti-apoptotic) compounds and SARS-CoV-2 protease

enzyme that obtained from protein data bank (PDB:5R7Z) using version 2014.09 of Molecular Operating Environment (MOE®) software and for validation of the method we used HWH as reference. The theoretical prediction results obtained from the molecular docking study were found to be a good illustration of observed SARS-CoV-2 protease inhibition activity.

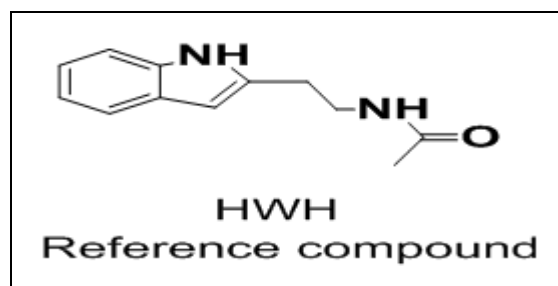


FIG. 2: A REFERENCE COMPOUND FOR PREDICTION THE BINDING INTERACTIONS BETWEEN ALL REPORTED CASPASE INHIBITOR (ANTI-APOPTOTIC) COMPOUNDS AND SARS-COV PROTEASE ENZYME

All studied compounds were successfully docked into the active site of the SARS-CoV protease enzyme. The binding free energies from the major docked poses are listed in **Table 1**, and the most favorable poses of the tested compounds are shown in **Fig. 2-15**. Most of the tested compounds have a high binding of the reference compound HWH is completely consistent with the mode of action of tested anti-apoptotic compounds. The 2D & 3D diagrams showed a crucial binding ARG298 with phenyl ring functionality. However, compounds 2-5, 7, 8, 10-13 showed greater binding as well as docking scores than the reference. Docking Results

with SARS-CoV protease revealed that all of the tested compounds show a good binding with ARG298 amino acid residue in addition to several interactions comparable to that of the reference HWH. Compounds 9 **Fig. 10** exhibited the same interaction with the conserved hydrophobic interaction (Pi-H) with ARG298 as HWH, both compounds 10 and 13 possess the greatest interaction amongst the tested compounds to interact with the same amino acid with additional hydrogen bonding with MET6 amino acid residue and hydrogen bonding with GLY302 and THR304 **Fig. 11 and 14**.

Although compounds 2, 4, 5, 7, and 11 showed hydrogen bonding with MET6 amino acid residue, besides, compounds 4, 11, and 12 exhibited hydrogen bonding interaction with CYS300, while compounds 1 and 3 only showed interaction with TYR154 **Fig. 2-15**. On the other hand, compound 6 **Fig. 9** dismissed hydrogen binding interactions with the amino acid residue ARG 298, explaining its weak activity, and compounds 5 and 8 kept only hydrogen bond interaction with SER1 **Fig. 9**.

TABLE 2: MOLECULAR DOCKING DATA FOR COMPOUNDS 1-13 AND HWH IN SARS-COV-2 ACTIVE SITE (PDB ID 5R7Z)

Code	S. score	Interaction with amino acid residue	Distance (Å)	ΔG (kcal/mol) ^a
1	-6.439	hydrogen bonding (H-acceptor) with TYR154	3.10	-0.8
		hydrophobic interaction (Pi-H) with ARG298	4.30	-2.5
2	-7.207	hydrogen bonding (H-donor) with MET6	3.34	-2.9
		hydrophobic interaction (Pi-H) with ARG298	4.39	-0.6
		hydrophobic interaction (Pi-H) with ARG298	4.08	-2.5
3	-7.500	hydrogen bonding (H-acceptor) with TYR154	3.10	-0.8
		hydrophobic interaction (Pi-H) with ARG298	4.30	-2.5
4	-7.050	hydrogen bonding (H-donor) with CYS300	3.21	-2.1
		hydrogen bonding (H-donor) with MET6	3.69	-1.6
		hydrophobic interaction (Pi-H) with ARG298	4.41	-2.7
5	-6.790	hydrogen bonding (H-donor) with MET6	3.30	-1.7
		hydrogen bonding (H-donor) with MET6	3.48	-0.6
		hydrophobic interaction (Pi-H) with SER1	4.48	-0.7
		hydrophobic interaction (Pi-H) with ARG298	4.07	-2.3
6	-5.811	hydrogen bonding (H-donor) with MET6	4.08	-0.5
		hydrogen bonding (H-donor) with VAL303	3.10	-0.7
		hydrogen bonding (H-donor) with GLY2	2.84	-5.9
7	-7.461	hydrogen bonding (H-donor) with MET6	3.62	-1.4
		hydrophobic interaction (Pi-H) with ARG298	4.56	-1.3
8	-7.412	hydrophobic interaction (Pi-H) with SER1	3.01	-0.9
		hydrophobic interaction (Pi-H) with ARG298	4.38	-2.7
9	-6.377	hydrophobic interaction (Pi-H) with ARG298	4.03	-1.8
		hydrophobic interaction (Pi-H) with ARG298	4.03	-1.8
10	-8.775	hydrogen bonding (H-donor) with MET6	3.52	-1.4
		hydrogen bonding (H-acceptor) with GLY302	3.16	-0.9
		hydrophobic interaction (Pi-H) with ARG298	3.99	-2.0
11	-7.255	hydrogen bonding (H-donor) with MET6	3.40	-2.1

		hydrogen bonding (H-donor) with CYS300	4.34	-0.8
12	-7.839	hydrophobic interaction (Pi-H) with ARG298	4.40	-1.8
		hydrogen bonding (H-acceptor) with ARG298	3.33	-0.8
		hydrogen bonding (H-acceptor) with GLY302	3.23	-1.1
		hydrophobic interaction (Pi-H) with CYS300	4.13	-1.4
13	-8.067	hydrogen bonding (H-donor) with MET6	3.34	-1.4
		hydrogen bonding (H-donor) with MET6	3.84	-0.6
		hydrophobic interaction (Pi-H) with ARG298	4.04	-2.6
		hydrophobic interaction (Pi-H) with THR304	3.85	-0.9
14	-6.507	hydrophobic interaction (Pi-H) with ARG298	4.05	-1.2

ΔG (Kcal/mole) a; the binding free energies

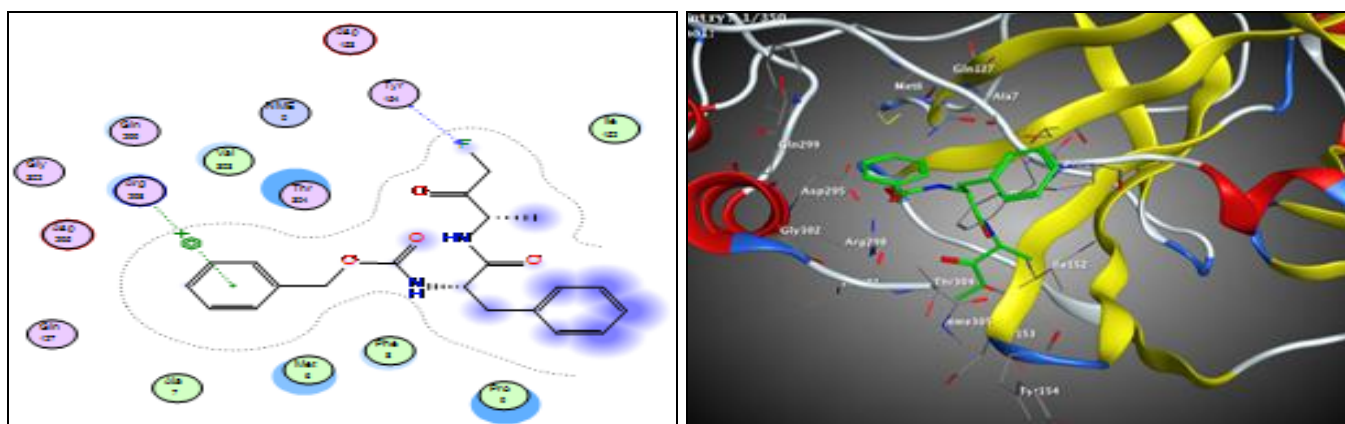


FIG. 3: THE BINDING MODE OF COMPOUND 1 INTERACTED WITH THE SARS-COV-2 ACTIVE SITE (PDB ID 5R7Z) IS SHOWN AS 2D AND 3D DIAGRAMS

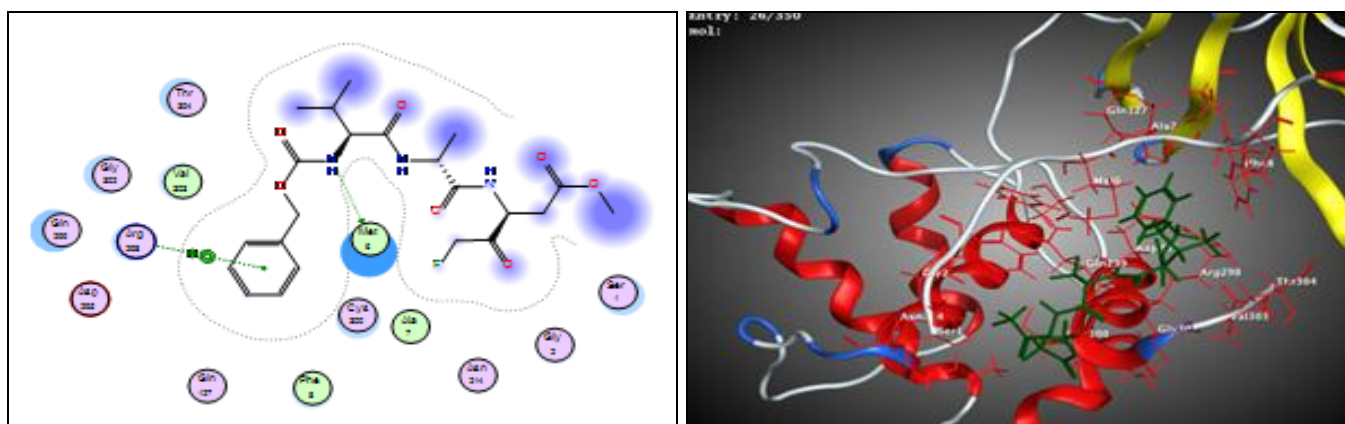


FIG. 4: THE BINDING MODE OF COMPOUND 2 INTERACTED WITH THE SARS-COV-2 ACTIVE SITE (PDB ID 5R7Z) IS SHOWN AS 2D AND 3D DIAGRAMS

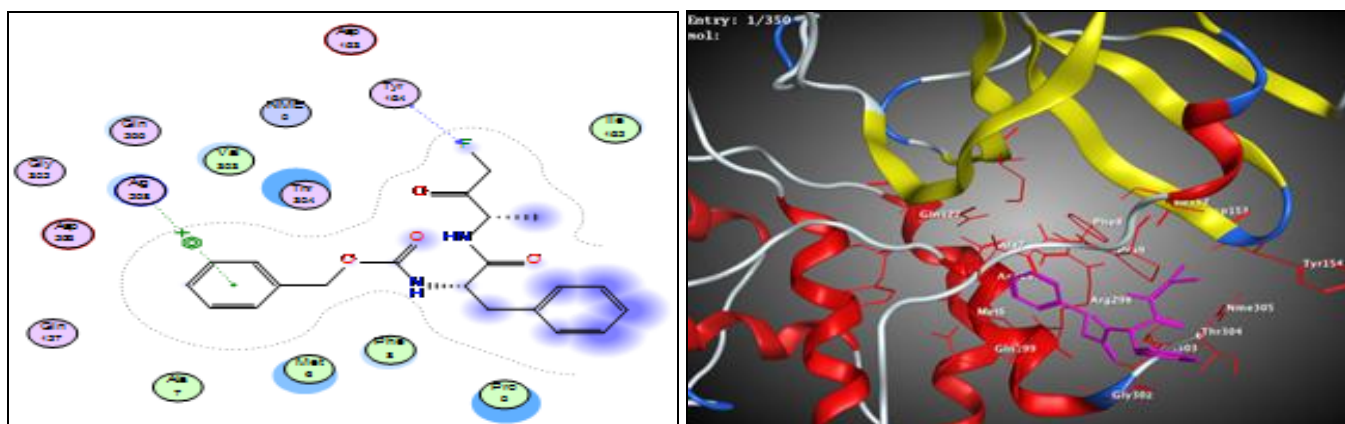


FIG. 5: THE BINDING MODE OF COMPOUND 3 INTERACTED WITH THE SARS-COV-2 ACTIVE SITE (PDB ID 5R7Z) IS SHOWN AS 2D AND 3D DIAGRAMS

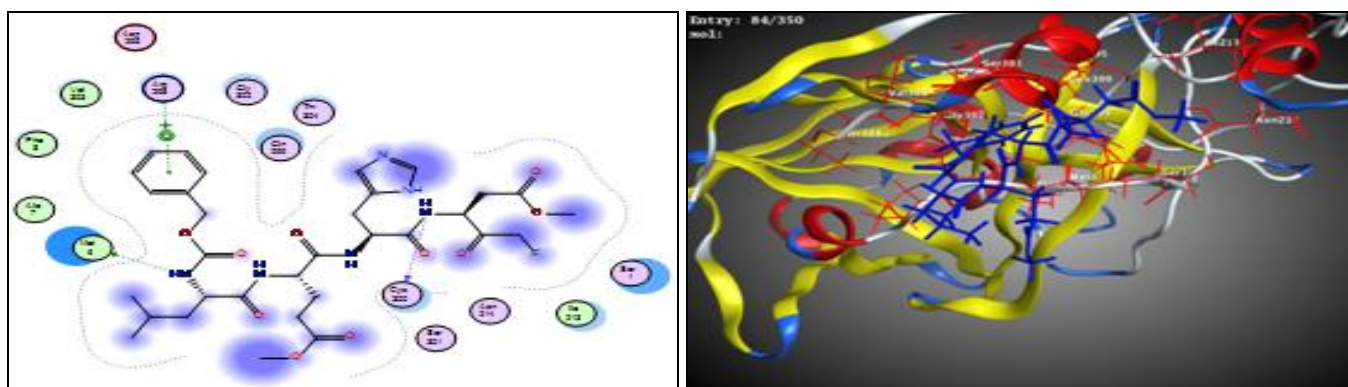


FIG. 6: THE BINDING MODE OF COMPOUND 4 INTERACTED WITH THE SARS-COV-2 ACTIVE SITE (PDB ID 5R7Z) IS SHOWN AS 2D AND 3D DIAGRAMS

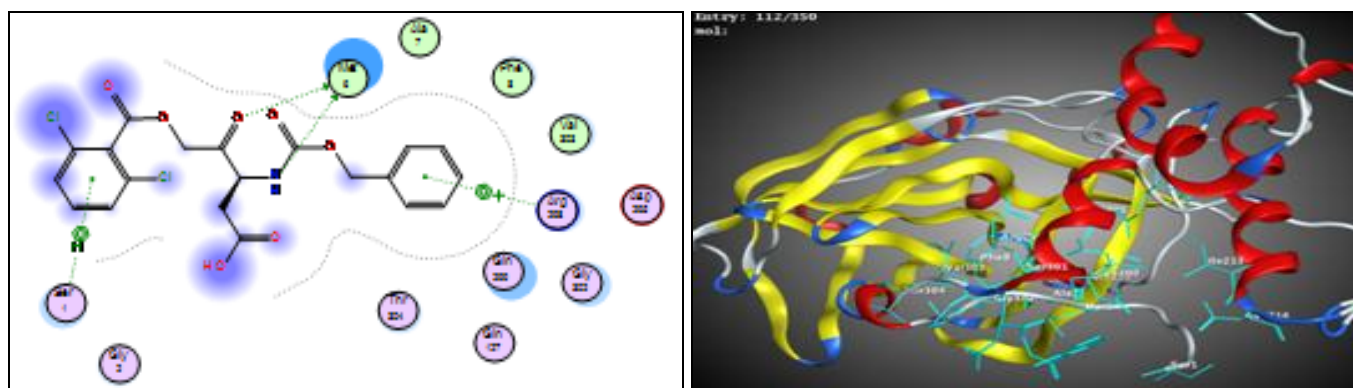


FIG. 7: THE BINDING MODE OF COMPOUND 5 INTERACTED WITH THE SARS-COV-2 ACTIVE SITE (PDB ID 5R7Z) IS SHOWN AS 2D AND 3D DIAGRAMS

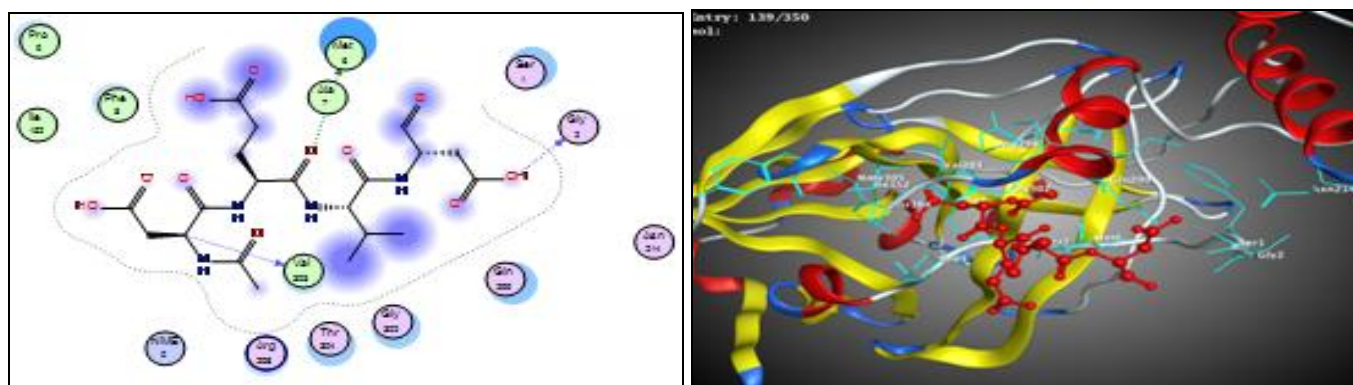


FIG. 8: THE BINDING MODE OF COMPOUND 6 INTERACTED WITH THE SARS-COV-2 ACTIVE SITE (PDB ID 5R7Z) IS SHOWN AS 2D AND 3D DIAGRAMS

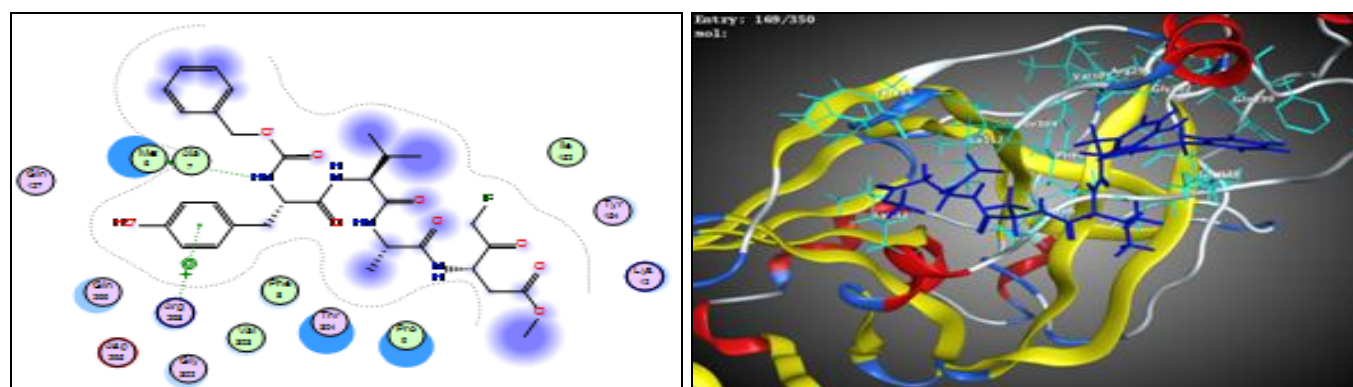


FIG. 9: THE BINDING MODE OF COMPOUND 7 INTERACTED WITH THE SARS-COV-2 ACTIVE SITE (PDB ID 5R7Z) IS SHOWN AS 2D AND 3D DIAGRAMS

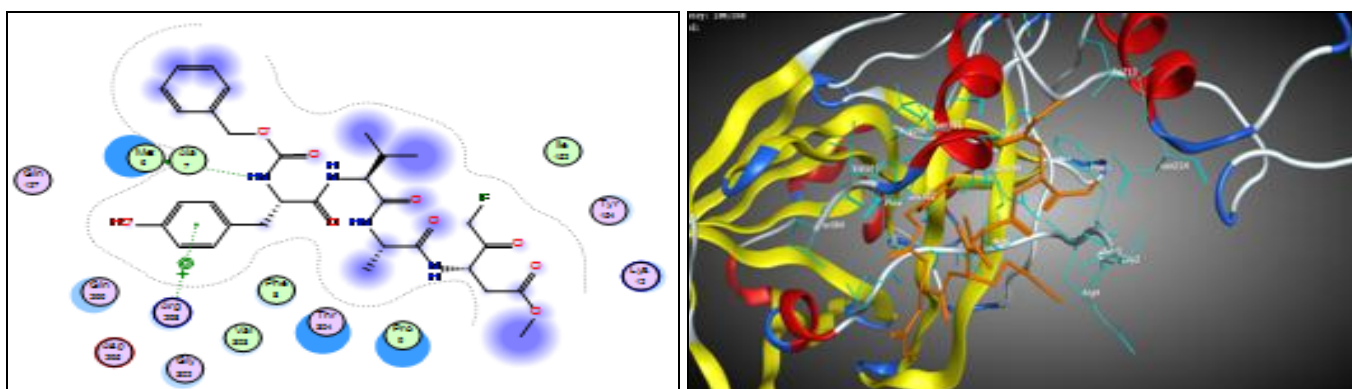


FIG. 10: THE BINDING MODE OF COMPOUND 8 INTERACTED WITH THE SARS-COV-2 ACTIVE SITE (PDB ID 5R7Z) IS SHOWN AS 2D AND 3D DIAGRAMS

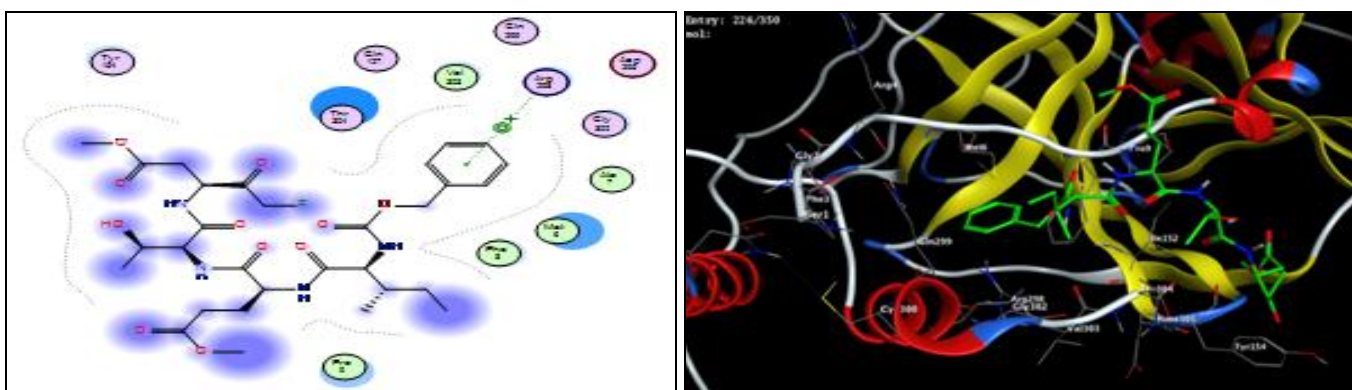


FIG. 11: THE BINDING MODE OF COMPOUND 9 INTERACTED WITH THE SARS-COV-2 ACTIVE SITE (PDB ID 5R7Z) IS SHOWN AS 2D AND 3D DIAGRAMS

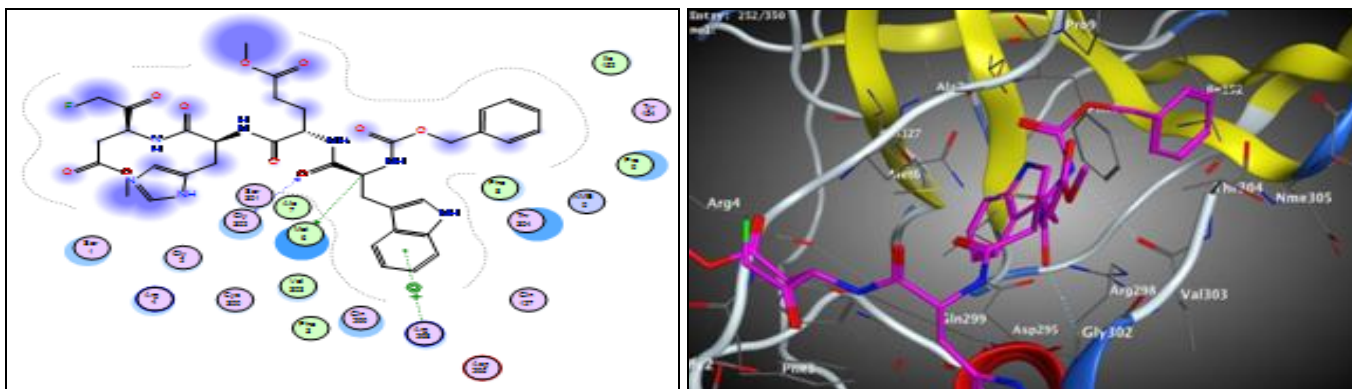


FIG. 12: THE BINDING MODE OF COMPOUND 10 INTERACTED WITH THE SARS-COV-2 ACTIVE SITE (PDB ID 5R7Z) IS SHOWN AS 2D AND 3D DIAGRAMS

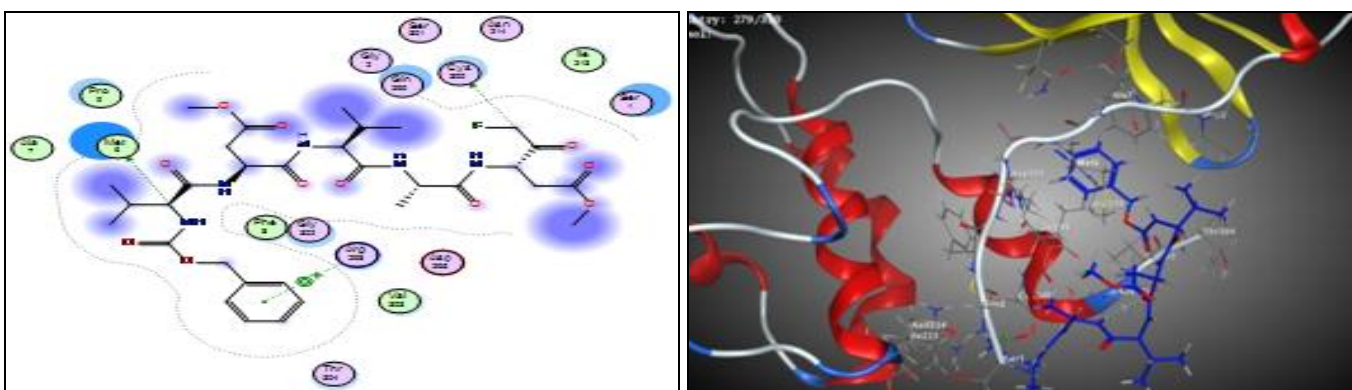


FIG. 13: THE BINDING MODE OF COMPOUND 11 INTERACTED WITH THE SARS-COV-2 ACTIVE SITE (PDB ID 5R7Z) IS SHOWN AS 2D AND 3D DIAGRAMS

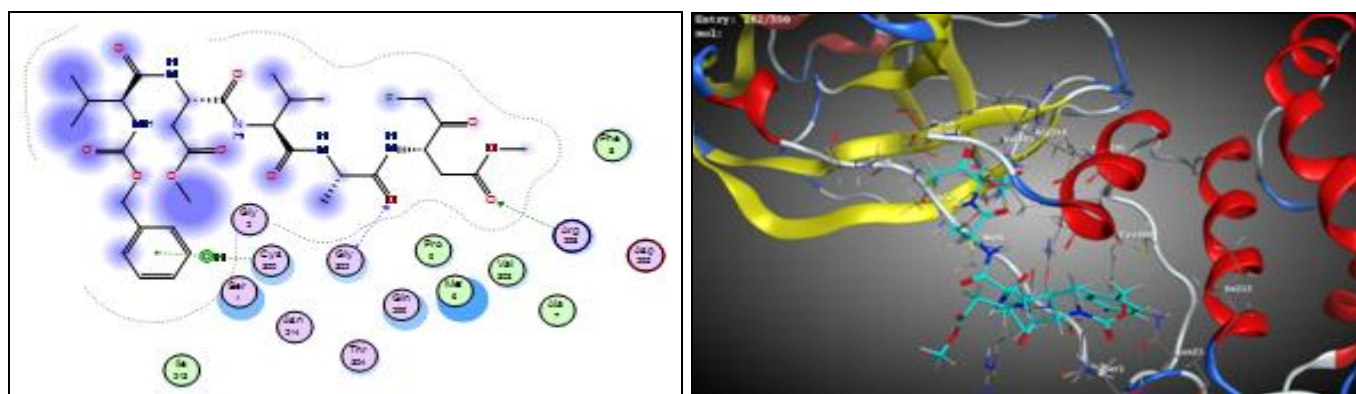


FIG. 14: THE BINDING MODE OF COMPOUND 12 INTERACTED WITH THE SARS-COV-2 ACTIVE SITE (PDB ID 5R7Z) IS SHOWN AS 2D AND 3D DIAGRAMS

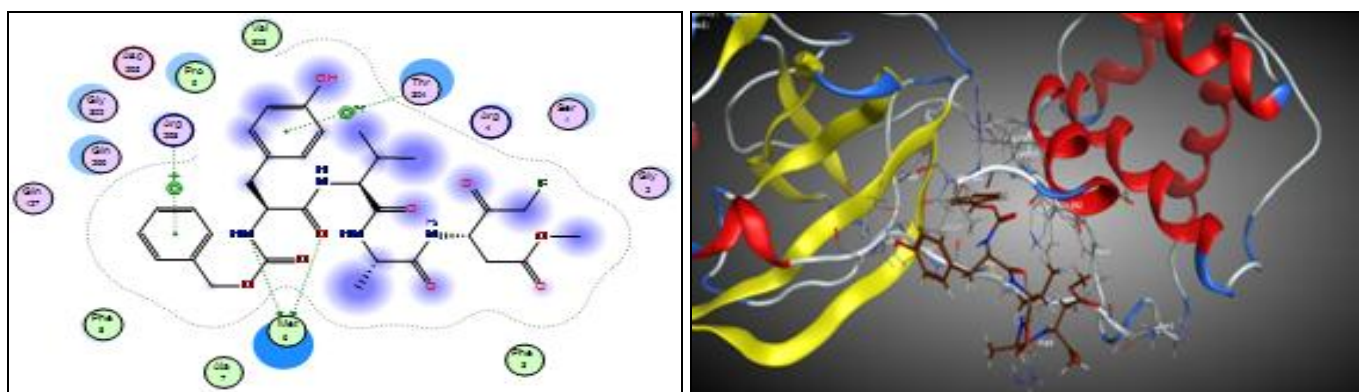


FIG. 15: THE BINDING MODE OF COMPOUND 13 INTERACTED WITH THE SARS-COV-2 ACTIVE SITE (PDB ID 5R7Z) IS SHOWN AS 2D AND 3D DIAGRAMS

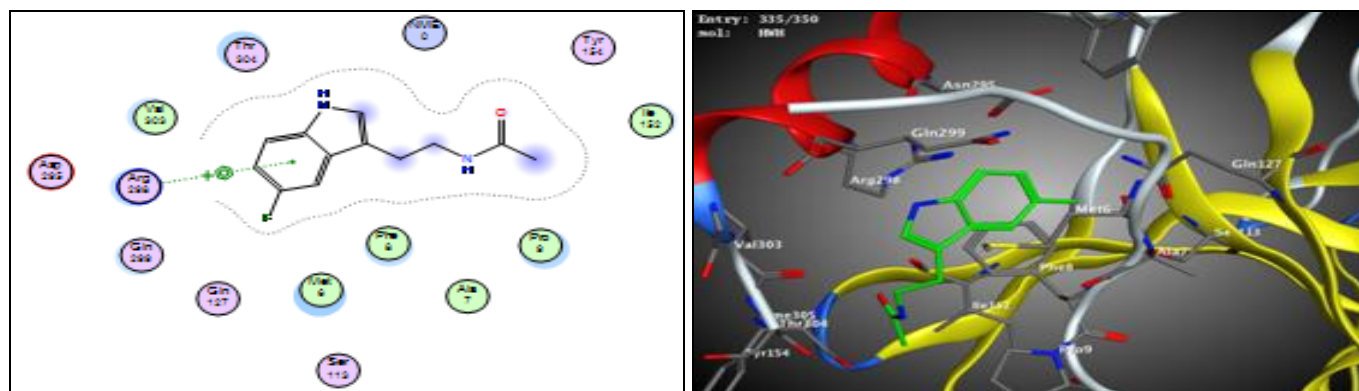


FIG. 16: THE BINDING MODE OF COMPOUND 14 INTERACTED WITH THE SARS-COV-2 ACTIVE SITE (PDB ID 5R7Z) IS SHOWN AS 2D AND 3D DIAGRAMS

Computational Analysis:

Prediction of Physicochemical Properties, Pharmacokinetics and Drug-Likeness Profile *in-Silico*:

Because of the costs required for the production of a new drug, in addition to inappropriate ADME parameters (distribution, excretion, absorption, and metabolism), design and applied new drugs is considered to be complicated. Therefore, evaluating the pharmacokinetic properties of a new drug is a critical step in the process of drug development and may lead directly to optimizing efforts to recover analogs⁸².

Currently, the most promising compounds can be picked *in-silico* ADMET screens, reducing the chance of degradation of drugs in late stages⁸³. To achieve a desired *in-vivo* response, it should be balance between pharmacodynamics and pharmacokinetic properties. Further, information about regimen and drug dose is given by the prediction of brain penetration, volume of distribution, oral bioavailability, and clearance⁸⁴. Many parameters such as drug solubility S, partition coefficients, polar surface PSA, cell permeability, human intestinal absorption HIA and

drug-likeness score have been studied during virtual screening methods. An available orally drug elected in agreement with Lipinski's rule if the molecular weight is less than 500 and LogP is not higher than 5, the number of hydrogen bond acceptors is less than 10 and the number of donor hydrogen bond donors is less than 5⁸⁵.

The number of rotatable bonds reflects molecular flexibility that plays an important role in oral bioavailability and means less orally active in a flexible molecule. The number of hydrogen bonding groups has also been suggested as a consideration to substitute for the polar surface area (PSA) and also to measure the percentage absorption (% ABS) as it is inversely proportional to tPSA

$$\% \text{ ABS} = 109 - 0.345 \text{ tPSA.}$$

The higher oral bioavailability was exhibited by Compounds with tPSA of less than 140 A² and 10 or fewer rotatable bonds⁸⁴. Herein, we used Pre-ADMET⁸⁵, Molinspiration⁸⁶, Molsoft⁸⁷, and Swiss ADME software⁸² for predicting the pharmacokinetic parameters of the reported compounds. The results are shown in **Table 2, Fig. 17** A exhibit that compounds 1, 2 and 5 obey the Lipinski's rule with LogP values from 1.76 to 3.17 (<5), aMW range from 386.42 to 467.49 (<500) and HBD from 2 to 5 (≤ 5) and HBA from 5 to 7 (<10). They would theoretically show a strong oral absorption and this property cannot be attributed to variations in their bioactivity. Besides, the topological PSA values of the compounds ring between⁸⁴. 50 and 119.00A² (< 140A²) and the corresponding percentage oral absorption was between⁸⁰, 54 and 60, 73% exhibit strong permeability, absorption and transport across biological membrane.

Furthermore, the drug-likeness model score and solubility for compounds was confirmed by Mol soft software **Table 3, Fig. 17B**. Aqueous solubility can change the absorption and distribution characteristics. The more positive drug-likeness model scores, the more likely it is to be a drug molecule; these compounds have fulfilled their solution ability specifications at values between 1.80 and 5.43 mg / l (above 0.0001 mg / L). Positive model-scores (0.07 and 0.29, respectively) were anticipated for compounds 3 and 11, while that for other compounds was negative (0.38 to -1.74). Additionally, the following pharmacokinetic parameters were experimented *in-silico* using Pre-ADMET software; blood-brain barrier partition coefficient (BBB), cytochrome inhibition of cytochrome P4502D6 (CYP2D6), Caco2, coefficient (human colon adenocarcinoma), MDCK (Madin-Darby canine kidney cells) permeability coefficient, human intestinal absorption (HIA) and human plasma-protein binding (PPB).

The results of the ADME parameters are shown in **Table 4 Fig. 17C**, findings from compounds with moderate CNS absorption ranges between 0.0324858 and 0.165928 (≤ 0.1); investigated compounds exhibited medium to low cell permeability in Caco-2 the MDCK models range from 13.105, 20.908 nm/s, and 0.043 to 1.14061 nm/s, respectively.

This is aligned with non-inhibitors of the CYP2D6 enzyme and thus may pretend no interactions with CYP2D6 inhibitors and/or inducers. Furthermore, they showed high human intestinal absorption values, 31.582 to 80.537% ($\leq 80\%$), indicating very well-absorbed compounds. The examined compounds were found to be highly-bound to human plasma proteins from 22.99 to 91.41%.

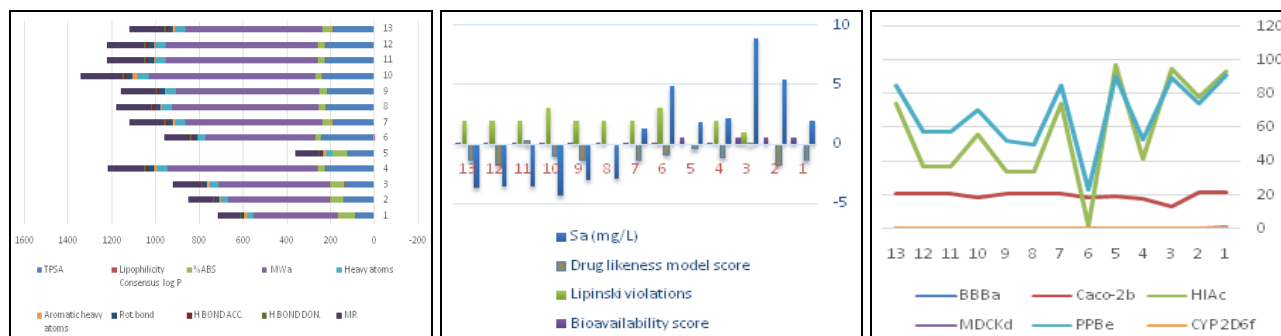


FIG. 17: ANALYSIS OF THE PHYSICOCHEMICAL PROPERTIES OF ANTI-APOPTOTIC COMPOUNDS 1-13 DISPLAYED IN TERMS OF (A) LIPOPHILICITY PARAMETERS, (B) LIPINSKI DRUG-LIK` ENESS

TABLE 3: PHYSICOCHEMICAL AND LIPOPHILICITY OF THE TARGET COMPOUNDS USING SWISSADME & MOLINSPIRATION SOFTWARE PHYSICOCHEMICAL PROPERTIES, (C) ADME DATA

Code	% ABS ^d	TPSA ^c (A2)	MR ^b	H-bond Don.	H-bond Acc.	Rot. Bond	Aromatic Heavy Atoms	Heavy Atoms	MW ^a g/mol	Lipophilicity Consensus Log P
1	80.53	84.50	102.08	2	5	12	12	28	386.42	2.80
2	60.73	139.90	115.53	3	8	17	6	33	467.49	1.76
3	62.53	134.69	128.90	3	9	13	16	37	513.49	3.02
4	31.72	223.98	170.10	5	12	27	11	49	690.72	1.30
5	67.94	119.00	107.52	2	7	12	12	30	454.26	3.17
6	24.35	245.37	115.78	7	11	20	0	35	502.47	-1.21
7	43.72	189.23	159.46	5	10	22	12	45	630.66	2.20
8	32.55	221.60	159.56	4	13	27	6	47	668.66	1.27
9	34.64	215.53	159.43	5	12	26	6	46	654.68	1.37
10	26.28	239.77	192.02	6	12	27	20	55	763.77	1.97
11	31.58	224.40	170.89	5	12	27	6	49	695.73	1.60
12	31.58	224.40	170.89	5	12	27	6	49	695.73	1.60
13	43.72	189.23	159.46	5	10	22	12	45	630.66	2.20

TABLE 4: LIPINSKI DRUG-LIKENESS OF THE TARGET COMPOUNDS USING MOLSOFT & SWISSADME SOFTWARE

Code	S ^a (mg/L)	Drug Likeness Model Score	Lipinski Violations	Bioavailability Score
1	1.92	-1.34	0	0.55
2	5.43	-1.74	0	0.55
3	8.92	0.07	1	0.56
4	2.21	-1.08	2	0.17
5	1.80	-0.38	0	0.56
6	4.84	-0.83	3	0.11
7	1.26	-1.32	2	0.17
8	-2.87	-1.48	2	0.17
9	-3.02	-1.33	2	0.17
10	-4.30	-0.95	3	0.17
11	-3.60	0.29	2	0.17
12	-3.60	-1.74	2	0.17
13	-3.70	-1.32	2	0.17

^aS: solubility ^aMW, molecular weight; ^bMR, molar refractivity; ^cTPSA, topological polar surface area; ^d% ABS: percentage of absorption.

TABLE 5: ADME DATA OF TESTED COMPOUNDS CALCULATED USING PREADMET SOFTWARE

Code	Pharmacokinetics					
	BBB ^a	Caco-2 ^b	HIA ^c	MDCK ^d	PPB ^e	CYP 2D6 ^f
1	0.165928	21.4175	94.001261	1.14061	91.412128	Non
2	0.0331208	21.0447	78.532991	0.0586783	74.155834	Non
3	0.100202	13.1055	95.657838	0.0450151	89.979583	Non
4	0.0348432	17.759	41.798342	0.0437101	53.006657	Non
5	0.425746	18.8316	97.582863	0.0859193	90.693978	Non
6	0.0578949	18.5763	1.948532	0.190423	22.992702	Non
7	0.0482086	20.908	74.296643	0.0434857	84.906348	Non
8	0.0541519	20.4361	33.985961	0.0437966	49.758655	Non
9	0.0405691	20.7373	34.427314	0.0464115	52.172462	Non
10	0.0337179	18.4563	56.272394	0.0436436	70.419827	Non
11	0.0324858	20.8217	37.273750	0.0450741	57.289514	Non
12	0.0324858	20.8217	37.273750	0.0450741	57.289514	Non
13	0.0482086	20.908	74.296643	0.0434857	84.906348	Non

^aBBB: blood-brain barrier penetration; ^bCACO-2: permeability through cells derived from human colon adenocarcinoma; ^cHIA: percentage human intestinal absorption; ^dMDCK: permeability through Madin-Darby canine kidney cells; ^ePPB: plasma protein binding; ^fCYP2D6: cytochrome P450 2D6

CONCLUSION: The theoretical predictions results obtained from the molecular docking study were found to be a good illustration of observed SARS-CoV protease inhibition activity that plays a key role in apoptosis. The 2D & 3D diagrams showed a crucial binding ARG298 with phenyl ring functionality; however, compounds 2-5, 7, 8, 10-13 showed greater binding as well as docking scores

than the reference. On the other hand, SARS-CoV-2 protease revealed that all the tested compounds show a good binding with ARG298 amino acid residue in addition to several interactions comparable to that of the reference HWH.

ACKNOWLEDGEMENT: The authors are thankful to Ahmed M. R. Eisa, Minia, Egypt for his efforts in reviewing the linguistic errors of Manuscript and DR Mahmoud said, faculty of pharmacy tanta university for check the plagiarism for our manuscript.

CONFLICTS OF INTEREST: We declare that we have no conflicts of interest.

REFERENCES:

- Rabi FA, Al Zoubi MS, Kasasbeh GA, Salameh DM and Al-Nasser AD: SARS-CoV-2 and Corona virus Disease 2019: What We Know So Far. *Pathog Basel Switz* 2020; 9.
- Coronavirus Update (Live): 65,464,093 Cases and 1,510,350 Deaths from COVID-19 Virus Pandemic - Worldometer [Internet]. [cited 2020 Dec 4]. Available from: <https://www.worldometers.info/coronavirus/>
- Weiss SR and Leibowitz JL: Coronavirus Pathogenesis. In: Maramorosch K, Shatkin AJ and Murphy FA: *Advances in Virus Research*. Academic Press 2011: 85-164.
- Ye ZW, Yuan S, Yuen KS, Fung SY, Chan CP and Jin DY: Zoonotic origins of human coronaviruses. *International Journal of Biological Sciences* 2020; 16(10): 1686.
- Song Z, Xu Y, Bao L, Zhang L, Yu P, Qu Y, Zhu H, Zhao W, Han Y and Qin C: From SARS to MERS, thrusting coronaviruses into the spotlight. *Viruses* 2019; 11(1): 59.
- Lin L, Lu L, Cao W and Li T: Hypothesis for potential pathogenesis of SARS-CoV-2 infection—a review of immune changes in patients with viral pneumonia. *Emerg Microbes Infect* 2020; 9: 727–32.
- Tan L, Wang Q, Zhang D, Ding J, Huang Q and Tang YQ: Lymphopenia predicts disease severity of COVID-19: a descriptive and predictive study. *Signal Transduction and Targeted Therapy*. Springer Nature 2020; 1–3.
- Huang Y, Dai H and Ke R: Principles of robust innate immune response to viral infections: a multiplex network analysis. *Frontiers in Immunology* 2019; 10: 1736.
- Zhao Q, Meng M, Kumar R, Wu Y, Huang J and Deng Y: Lymphopenia is associated with severe coronavirus disease 2019 (COVID-19) infections: A systemic review and meta-analysis. *Int J Infect Dis* 2020; 96: 131–5.
- Li G, Fan Y, Lai Y, Han T, Li Z, Zhou P, Pan P, Wang W, Hu D, Liu X and Zhang Q: Coronavirus infections and immune responses. *Journal of Medical Virology* 2020; 92(4): 424-32.
- Rokni M, Ghasemi V and Tavakoli Z: Immune responses and pathogenesis of SARS-CoV-2 during an outbreak in Iran: Comparison with SARS and MERS. *Rev Med Virol* 2020; 30: 2107.
- Yang D, Chu H, Hou Y, Chai Y, Shuai H, Lee AC, Zhang X, Wang Y, Hu B, Huang X and Yuen TT: Attenuated interferon and proinflammatory response in SARS-CoV-2-infected human dendritic cells is associated with viral antagonism of STAT1 phosphorylation. *The Journal of Infectious Diseases* 2020; 222(5): 734-45.
- Mehta P, McAuley DF, Brown M, Sanchez E, Tattersall RS and Manson JJ: COVID-19: consider cytokine storm syndromes and immunosuppression. *The Lancet* 2020; 395: 1033–4.
- Zhang T, Sun LX and Feng RE: Comparison of clinical and pathological features between severe acute respiratory syndrome and coronavirus disease 2019. *Zhonghua jie he he hu xi za zhi= Zhonghua Jiehe he Huxi Zazhi= Chinese Journal of Tuberculosis and Respiratory Diseases* 2020; 43: 40.
- Melenotte C, Silvin A, Goubet AG, Lahmar I, Dubuisson A, Zumla A, Raoult D, Merad M, Gachot B, Hénon C and Solary E: Immune responses during COVID-19 infection. *Onco Immunology* 2020; 9(1): 1807836.
- Chousterman BG, Swirski FK and Weber GF: Cytokine storm and sepsis disease pathogenesis. *Semin Immunopathol* 2017; 39: 517–28.
- Zhao C and Zhao W: NLRP3 Inflammasome A Key Player in Antiviral Responses. *Front Immunol* 2020; 11: 211.
- Ye Q, Wang B and Mao J: The pathogenesis and treatment of the Cytokine Storm in COVID-19. *Journal of Infection* 2020; 80(6): 607-13.
- Tan HY, Yong YK, Shankar EM, Paukovics G, Ellegård R and Larsson M: Aberrant Inflammasome Activation Characterizes Tuberculosis-Associated Immune Reconstitution Inflammatory Syndrome. *J Immunol* 2016; 196: 4052–63.
- Yang D, Chu H, Hou Y, Chai Y, Shuai H, Lee AC, Zhang X, Wang Y, Hu B, Huang X and Yuen TT: Attenuated interferon and proinflammatory response in SARS-CoV-2-infected human dendritic cells is associated with viral antagonism of STAT1 phosphorylation. *The Journal of Infectious Diseases* 2020; 222(5): 734-45.
- Yang D, Chu H, Hou Y, Chai Y, Shuai H, Lee AC, Zhang X, Wang Y, Hu B, Huang X and Yuen TT: Attenuated interferon and proinflammatory response in SARS-CoV-2-infected human dendritic cells is associated with viral antagonism of STAT1 phosphorylation. *The Journal of Infectious Diseases* 2020; 222(5): 734-45.
- Grimes JM and Grimes KV: p38 MAPK inhibition: A promising therapeutic approach for COVID-19. *Journal of Molecular and Cellular Cardiology* 2020; 16.
- Negróni A, Colantoni E, Cucchiara S and Stronati L: Necroptosis in Intestinal Inflammation and Cancer: New Concepts and Therapeutic Perspectives. *Biomolecules* 2020; 10(10): 1431.
- Nainu F, Shiratsuchi A and Nakanishi Y: Induction of apoptosis and subsequent phagocytosis of virus-infected cells as an antiviral mechanism. *Frontiers in Immunology*. Frontiers Media S.A 2017; 1220.
- Chau AS, Weber AG, Maria NI, Narain S, Liu A, Hajizadeh N, Malhotra P, Bloom O, Marder G and Kaplan B: The Longitudinal Immune Response to Coronavirus Disease 2019: Chasing the Cytokine Storm. *Arthritis & Rheumatology* 2020; 15.
- Lee JK, Kim J, Oh SJ, Lee EW and Shin OS: Zika Virus Induces Tumor Necrosis Factor-Related Apoptosis Inducing Ligand (TRAIL)-Mediated Apoptosis in Human Neural Progenitor Cells. *Cells* 2020; 9(11): 2487.
- Connolly PF and Fearnhead HO: Viral hijacking of host caspases: An emerging category of pathogen-host interactions. *Cell Death and Differentiation*. Nature Publishing Group 2017; 1401–10.
- James CD, Fontan CT and Morgan IM: Human papillomavirus 16 E6 and E7 synergistically repress innate immune gene transcription. *Mosphere* 2020; 5(1).

29. Kesavardhana S, Malireddi RS and Kanneganti TD: Caspases in Cell Death, Inflammation, and Pyroptosis. *Annual Review of Immunology* 2020; 38: 567-95.
30. Lai Y, Wang M, Cheng A, Mao S, Ou X, Yang Q, Wu Y, Jia R, Liu M, Zhu D and Chen S: Regulation of Apoptosis by Enteroviruses. *Frontiers in Microbiology* 2020; 11: 1145.
31. Navratil V, Lionnard L, Longhi S, Combet C and Aouacheria A: The severe acute respiratory syndrome coronavirus 2 (SARS-CoV-2) envelope (E) protein harbors a conserved BH3-like motif. *bioRxiv* 2020; 033522.
32. Cong Y, Ulasli M, Schepers H, Mauthe M, V'kovski P and Kriegenburg F: Nucleocapsid Protein Recruitment to Replication-Transcription Complexes Plays a Crucial Role in Coronaviral Life Cycle. *J Virol* 2019; 94.
33. Oh C, Kim Y and Chang KO: Caspase-mediated cleavage of nucleocapsid protein of a protease-independent porcine epidemic diarrhea virus strain. *Virus Res* 2020; 285: 198026.
34. Farrera-Soler L, Dagher JP, Barluenga S, Vadas O, Cohen P, Pagano S, Yerly S, Kaiser L, Vuilleumier N and Winssinger N: Identification of immunodominant linear epitopes from SARS-CoV-2 patient plasma. *PLoS One* 2020; 15(9): 0238089.
35. Farrera-Soler L, Dagher JP and Winssinger N: Identification of immunodominant linear epitopes from SARS-CoV-2 patient plasma. *PLoS One* 2020; 15(9): 0238089.
36. Kannan S, Ali PS, Sheeza A and Hemalatha K: COVID-19 (Novel Coronavirus 2019)-recent trends. *Eur Rev Med Pharmacol Sci* 2020; 24(4): 2006-11.
37. Ivanisenko NV, Seyrek K, Kolchanov NA, Ivanisenko VA and Lavrik IN: The role of death domain proteins in host response upon SARS-CoV-2 infection: modulation of programmed cell death and translational applications. *Cell Death Discovery* 2020; 6(1): 1-0.
38. Gatti P, Ilamathi HS, Todkar K and Germain M: Mitochondria Targeted Viral Replication and Survival Strategies Prospective on SARS-CoV-2. *Frontiers in Pharmacology* 2020; 11.
39. Amor S, Fernández Blanco L and Baker D: Innate immunity during SARS-CoV-2: evasion strategies and activation trigger hypoxia and vascular damage. *Clinical & Experimental Immunology* 2020; 202(2): 193-209.
40. Justin S, Rutz J, Maxeiner S, Chun FK, Juengel E and Blaheta RA: Bladder Cancer Metastasis Induced by Chronic Everolimus Application Can Be Counteracted by Sulforaphane *in-vitro*. *International Journal of Molecular Sciences* 2020; 21(15): 5582.
41. Neufeldt CJ, Cerikan B, Cortese M, Frankish J, Lee JY, Plociennikowska A, Heigwer F, Joecks S, Burkart SS, Zander DY and Gendarme M: SARS-CoV-2 infection induces a pro-inflammatory cytokine response through cGAS-STING and NF- κ B. *bioRxiv* 2020; 1.
42. Zhu H, Chen CZ, Sakamuru S, Simeonov A, Hall MD, Xia M, Zheng W and Huang R: Mining of high throughput screening database reveals AP-1 and autophagy pathways as potential targets for COVID-19 therapeutics. *arXiv preprint arXiv* 2020; 12242.
43. Lin Z, Gao Q, Qian F, Jinlian M, Lishi Z, Tian C, Yu Q, Zhenhua C, Ping W and Lin B: The nucleocapsid protein of SARS-CoV-2 abolished pluripotency in human induced pluripotent stem cells 2020; 26.
44. Oh C, Kim Y and Chang KO: Caspase-mediated cleavage of nucleocapsid protein of a protease-independent porcine epidemic diarrhea virus strain. *Virus Res* 2020; 198026.
45. Sarkar M and Saha S: Structural insight into the role of novel SARS-CoV-2 E protein: A potential target for vaccine development and other therapeutic strategies. *PLOS ONE* 2020; 15:0237300.
46. Schoeman D and Fielding BC: Coronavirus envelope protein: current knowledge. *Virol J* 2019; 16: 69.
47. Schoeman D and Fielding BC: Coronavirus envelope protein: current knowledge. *Virology Journal* 2019; 16(1): 1-22.
48. Yuan S, Zhang N, Xu L, Zhou L, Ge X, Guo X and Yang H: Induction of apoptosis by the nonstructural protein 4 and 10 of porcine reproductive and respiratory syndrome virus. *PLoS One* 2016; 11(6): 0156518.
49. Lippi A, Domingues R, Setz C, Outeiro TF and Krisko A: SARS-CoV-2: at the crossroad between aging and neurodegeneration. *Movement Disorders* 2020; 35(5): 716-20.
50. Castaño-Rodríguez C, Honrubia JM and Kochan G: Role of severe acute respiratory syndrome coronavirus viroporins E, 3a and 8a in replication and pathogenesis. *MBio* 2018; 9(3).
51. Connolly PF and Fearnhead HO: Viral hijacking of host caspases: An emerging category of pathogen-host interactions. *Cell Death and Differentiation*. Nature Publishing Group 2017; 1401-10.
52. Chen IY, Moriyama M, Chang MF and Ichinohe T: Severe Acute Respiratory Syndrome Coronavirus Viroporin 3a Activates the NLRP3 Inflammasome. *Front Microbiol* 2019; 10: 50.
53. Yuan X, Shan Y, Yao Z, Li J, Zhao Z and Chen J: Mitochondrial location of severe acute respiratory syndrome coronavirus 3b protein. *Mol Cells* 2006; 21:186-91.
54. Astuti I and Ysrafil: Severe Acute Respiratory Syndrome Coronavirus 2 (SARS-CoV-2): An overview of viral structure and host response. *Diabetes Metab Syndr* 2020; 14: 407-12.
55. Nelson CA, Pekosz A, Lee CA, Diamond MS and Fremont DH: Structure and Intracellular Targeting of the SARS-Coronavirus Orf7a Accessory Protein. *Structure* 2005; 13: 75-85.
56. Yao Z, Zheng Z, Wu K and Junhua Z: Immune environment modulation in pneumonia patients caused by coronavirus: SARS-CoV, MERS-CoV and SARS-CoV-2. *Aging (Albany NY)* 2020; 12: 7639-51.
57. Fielding BC, Gunalan V, Tan THP, Chou C-F, Shen S and Khan S: Severe acute respiratory syndrome coronavirus protein 7a interacts with hSGT. *Biochem Biophys Res Commun* 2006; 343: 1201-8.
58. Imre G: Cell death signalling in virus infection. *Cell Signal* 2020; 76: 109772.
59. Zhang L, Zhang L, Lin D, Sun X, Curth U and Drosten C: Crystal structure of SARS-CoV-2 main protease provides a basis for design of improved α -ketoamide inhibitors 2020; 3405: 1-9.
60. Panfoli I: Potential role of endothelial cell surface ectopic redox complexes in COVID-19 disease pathogenesis. *Clin Med (Lond)* 2020; 20: 146-7.
61. Robinson BA, Winkle JAV, McCune BT, Peters AM and Nice TJ: Caspase-mediated cleavage of murine norovirus NS1/2 potentiates apoptosis and is required for persistent infection of intestinal epithelial cells. *PLOS Pathogens* 2019; 15: 1007940.
62. Xia B and Kang X: Activation and maturation of SARS-CoV main protease 2011; 2: 282-90.
63. Zhang L, Zhang L, Lin D, Sun X, Curth U and Drosten C: Crystal structure of SARS-CoV-2 main protease provides a basis for design of improved α -ketoamide inhibitors. 2020; 3405: 1-9.

64. Severe acute respiratory syndrome coronavirus 3C-like protease-induced apoptosis Pathogens and Disease Oxford Academic [Internet]. [cited 2020 Sep 1]. Available from: <https://academic.oup.com/femspd/article/46/3/375/555171>
65. Ren L, Yang R, Guo L, Qu J, Wang J and Hung T: Apoptosis Induced by the SARS-Associated Coronavirus in Vero Cells Is Replication-Dependent and Involves Caspase. *DNA and Cell Biology* 2005; 24: 496–502.
66. Roscow O, Ganassin R, Garver K and Polinski M: Z-FA-FMK demonstrates differential inhibition of aquatic orthoreovirus (PRV), aquareovirus (CSRV), and rhabdovirus (IHNV) replication. *Virus Res* 2018; 244: 194–8.
67. Chauvier D, Ankri S, Charriat-Marlangue C, Casimir R and Jacotot E: Broad-spectrum caspase inhibitors: From myth to reality? *Cell Death and Differentiation*. Nature Publishing Group 2007; 14: 387–91.
68. Kim M, Hansen KK, Davis L, Van Marle G, Gill MJ and Fox JD: Z-FA-FMK as a novel potent inhibitor of reovirus pathogenesis and oncolysis *in-vivo*. *Antivir Ther* 2010; 15: 897–905.
69. Martin U, Jarasch N, Nestler M, Rassmann A, Munder T and Seitz S: Antiviral effects of pan-caspase inhibitors on the replication of coxsackievirus B3. *Apoptosis Int J Program Cell Death* 2007; 12: 525–33.
70. Blum SI and Tse HM: Innate Viral Sensor MDA5 and Coxsackievirus Interplay in Type 1 Diabetes Development. *Microorganisms* 2020; 8(7): 993.
71. Zhang J, Han Y, Shi H, Chen J, Zhang X and Wang X: Swine acute diarrhea syndrome coronavirus-induced apoptosis is caspase- and cyclophilin D- dependent. *Emerg Microbes Infect* 2020; 9: 439–56.
72. Terahara K, Iwabuchi R, Iwaki R, Takahashi Y and Tsunetsugu-Yokota Y: Substantial induction of non-apoptotic CD4 T-cell death during the early phase of HIV-1 infection in a humanized mouse model. *Microbes and Infection* 2020; 10.
73. Li BX, Zhang H, Liu Y, Li Y, Zheng JJ, Li WX, Feng K, Sun M and Dai SX: Novel pathways of HIV latency reactivation revealed by integrated analysis of transcriptome and target profile of bryostatin. *Scientific Reports* 2020; 10(1): 1-2.
74. Zhang J, Han Y, Shi H, Chen J, Zhang X and Wang X: Swine acute diarrhea syndrome coronavirus-induced apoptosis is caspase- and cyclophilin D- dependent. *Emerg Microbes Infect* 2020; 9: 439–56.
75. Kennedy S, Leroux MM, Simons A, Malve B, Devocelle M and Varbanov M: Apoptosis and autophagy as a turning point in viral–host interactions: the case of human norovirus and its surrogates. *Fut Viro* 2020; 15(3): 165-82.
76. Cai W, Wen H, Zhou Q, Wu L, Chen Y, Zhou H and Jin M: 14-Deoxy-11, 12-didehydroandrographolide inhibits apoptosis in influenza A (H5N1) virus-infected human lung epithelial cells via the caspase-9-dependent intrinsic apoptotic pathway which contributes to its antiviral activity. *Antiviral Research* 2020; 181: 104885.
77. Furukawa Y, Takasu A and Yura Y: Role of autophagy in oncolytic herpes simplex virus type 1-induced cell death in squamous cell carcinoma cells. *Cancer Gene Ther* 2017; 24: 393–400.
78. Pinggen M, Bryden SR, Pondeville E, Fazakerley JK, Graham GJ and Mckimmie CS: Host Inflammatory Response to Mosquito Bites Enhances the Severity of Arbovirus Infection Article Host Inflammatory Response to Mosquito Bites Enhances the Severity of Arbovirus Infection. *Immunity* 2016; 44: 1455–69.
79. Kofahi HM, Taylor NGA, Hirasawa K, Grant MD, Russell RS. Hepatitis C Virus Infection of Cultured Human Hepatoma Cells Causes Apoptosis and Pyroptosis in Both Infected and Bystander Cells *Sci Rep* 2016; 6.
80. Lippi A, Domingues R, Setz C, Outeiro TF and Krisko A: SARS-CoV-2: at the crossroad between aging and neurodegeneration. *Movement Disor* 2020; 35(5): 716-20.
81. Zhao M, Duan X, Wang Y, Gao L, Cao H and Li X: A novel role for PX, a structural protein of fowl adenovirus serotype 4 (FADV4), as an apoptosis-inducer in Leghorn Male hepatocellular cell. *Viruses* 2020; 12.
82. Daina A, Michielin O and Zoete V: Swiss ADME: a free web tool to evaluate pharmacokinetics, drug-likeness and medicinal chemistry friendliness of small molecules. *Scientific Reports* 2017; 7: 42717.
83. Van De Waterbeemd H and Gifford E: ADMET *in-silico* modelling: towards prediction paradise. *Nature reviews Drug Discovery* 2003; 2(3): 192-204.
84. Veber D, Johnson S, Cheng H, Smith B, Ward K and Kopple K: Differential Uptake and Selective Permeability of Fusarochromanone (FC101), a Novel Membrane Permeable Anticancer Naturally Fluorescent Compound in Tumor and Normal Cells. *J Med Chem* 2002; 45: 2615-23.
85. Rajanarendar E, Krishna SR, Nagaraju D, Reddy KG, Kishore B and Reddy Y: Environmentally benign synthesis, molecular properties prediction and anti-inflammatory activity of novel isoxazolo [5, 4-d] isoxazol-3-yl-aryl-methanones via vinylogous Henry nitroaldol adducts as synthons. *Bioorganic & Medicinal Chemistry Letters* 2015; 25(7): 1630-4.
86. Lagorce D, Reynes C, Camproux AC, Miteva MA, Sperandio O and Villoutreix BO: *In-silico* adme/tox predictions. *ADMET for Medicinal Chemists: A Practical Guide* Hoboken. New Jersey John Wiley & Sons Inc 2011: 29-124.
87. Wetzel S, Schuffenhauer A, Roggo S, Ertl P and Waldmann H: Cheminformatic analysis of natural products and their chemical space. *CHIMIA International Journal for Chemistry* 2007; 61(6): 355-60.
88. Bakht MA, Yar MS, Abdel-Hamid SG, Al Qasoumi SI, Samad A. Molecular properties prediction, synthesis and antimicrobial activity of some newer oxadiazole derivatives 2010; 45(12): 5862-69.

How to cite this article:

Zaki MMA, Ahmed YM and Abdelhafez MNE: Candidature of the synthetic caspase inhibitors as new anti-sars-cov-2 drug discovery, *in-silico* molecular docking. *Int J Pharm Sci & Res* 2021; 12(1): 104-19. doi: 10.13040/IJPSR.0975-8232.12(1).104-19.

All © 2013 are reserved by the International Journal of Pharmaceutical Sciences and Research. This Journal licensed under a Creative Commons Attribution-NonCommercial-ShareAlike 3.0 Unported License.

This article can be downloaded to **Android OS** based mobile. Scan QR Code using Code/Bar Scanner from your mobile. (Scanners are available on Google Playstore)